Atomistic models of LMRNMC Materials

Project ID ES: 193

Hakim Iddir

Voltage Fade Team

Annual Merit Review

Washington DC, June 16-20, 2014

Overview

Timeline

- Start: October 1, 2012
- End: Sept. 30, 2014
- Percent complete: 85%

Budget

- Voltage Fade project

Barriers

- Calendar/cycle life of lithium-ion cells being developed for PHEV and EV batteries that meet or exceed DOE/USABC goals

Partners

- ORNL
- NREL
- ARL
- JPL

Project Objectives - Relevance

Objectives:

LMRNMC cathode materials are modeled at the atomic scale to characterize the structure of the starting material and the mechanism of VF in cycled materials. We also identify and evaluate strategies for the design of high capacity, high energy-density, VF-free materials.

Approach:

We perform first-principles density functional theory (DFT) at the GGA+*U* level. Computational cells including up to several hundred atoms in the periodic unit are employed. This work is being coordinated with experimental efforts, including the synthesis and characterization groups.

Milestones:

- Evaluate the phase composition and atomic order in pristine LMRNMC composites.
- Investigate possible instabilities in Li_2MnO_3 and $LiCoO_2/Li_2MnO_3$ composite resulting from cycling (esp. first charge).
- Correlate local structures with experimental observations based on NMR, EXAFS, XPS, TEM and XRD.

$Li_2MnO_3 \bullet LiMO_2$ composites: simulations for M=Co

- Pristine material
- Simulation of first cycle

➔exploit expt. to eliminate degrees of freedom in simulation

[XAS(Croy et al. ES: 194), NMR (Key et al. ES 187), electrochem.]

Pristine material $Li_2MnO_3 \bullet LiCoO_2$

- First-principles calculations (GGA+U) of domains of different shapes and sizes

➔ Material phase-separates (at thermo. eq.)*

• Features of composite:

A. enhanced stability during delithiation (relative to pure phases)

B. Special properties of domain interfaces

➔ Focus on composite rather than Li_2MnO_3

*HI and RB, Chem. Mater. 2014

Pristine material $Li_2MnO_3 \bullet LiCoO_2$

- First-principles calculations (GGA+U) of domains of different shapes and sizes

➔ Material phase-separates (at thermo. eq.)*

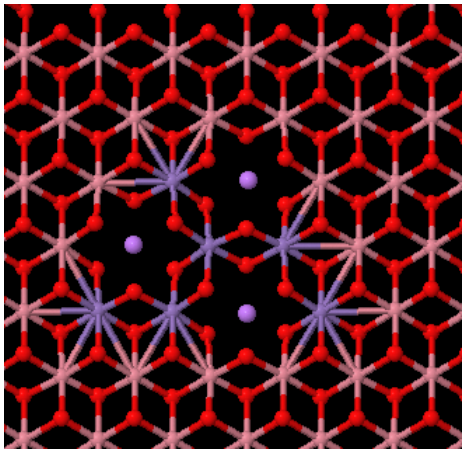

3 $LiMn_2$ units

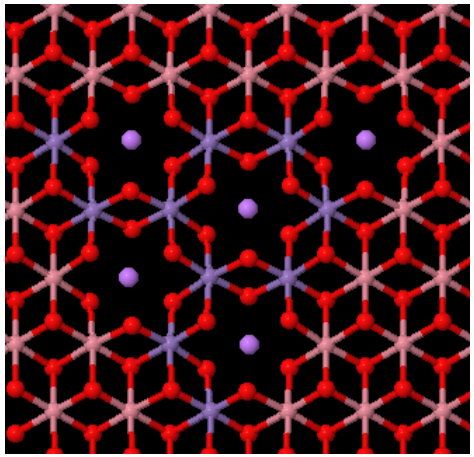

5 $LiMn_2$ units

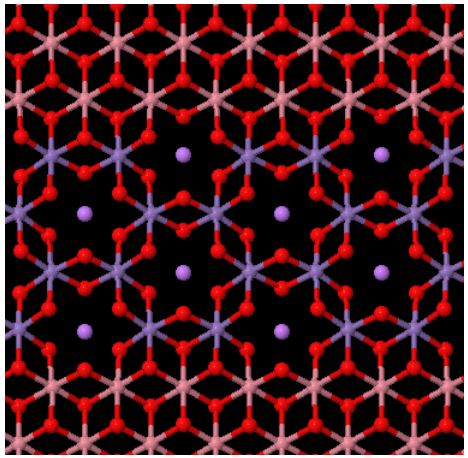

8 $LiMn_2$ units (thick ribbon)

*HI and RB, Chem. Mater. 2014

Domains in: $xLi(Li_{1/3}Mn_{2/3})O_2 \bullet (1\text{-}x)LiCoO_2$ x=1/16,…1

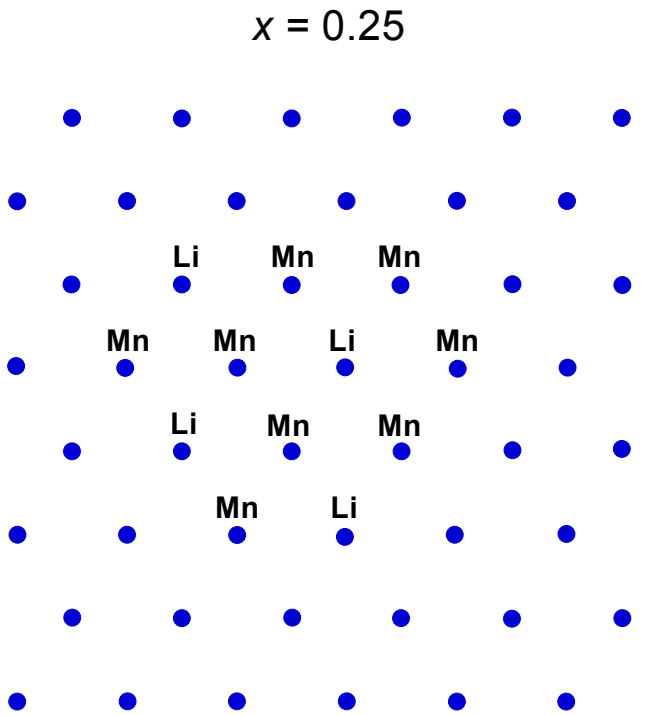

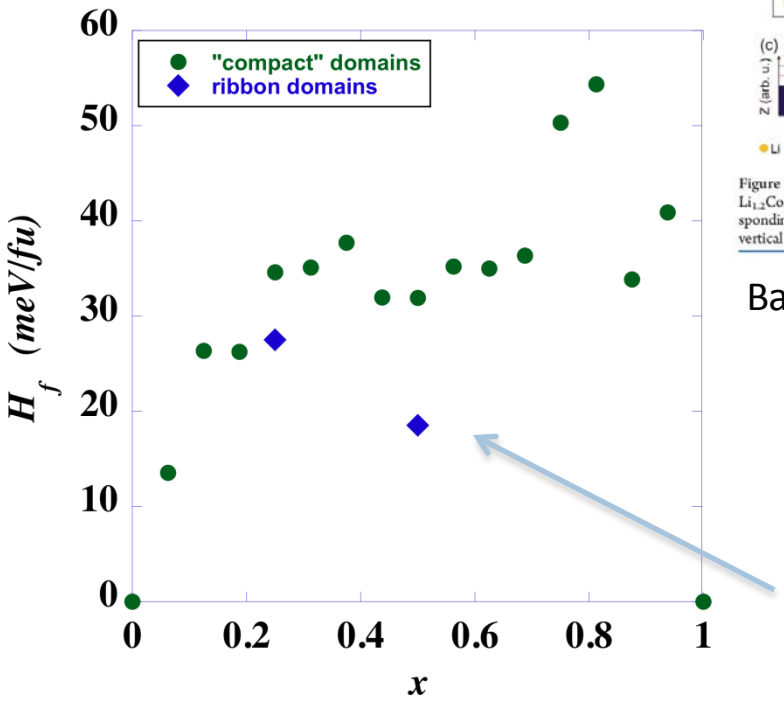

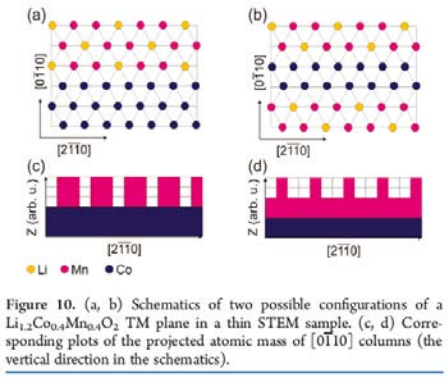

Figure 10. (a, b) Schematics of two possible configurations of a $Li_{1.2}Co_{0.4}Mn_{0.4}O_2$ TM plane in a thin STEM sample. (c, d) Corresponding plots of the projected atomic mass of [0$\bar{1}$10] columns (the vertical direction in the schematics).

Bareno J. et al. CM 2011

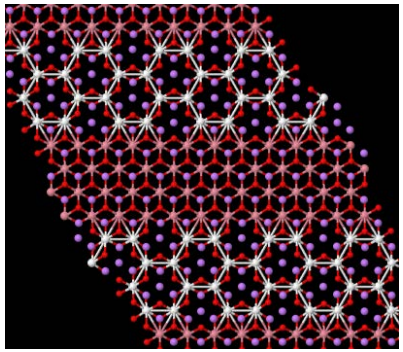

Phase Diagram: predict minute (<1%) solubility of 213 in layered matrix, based on calculations for MnCo model system

Question: Are the kinetics fast enough to accomplish the phase segregation?
→ Self diffusion of M in $LiMO_2$ (supplementary slides)

*HI and RB, Chem. Mater. 2014

c-axis stress induced by delithiation of Li-layer

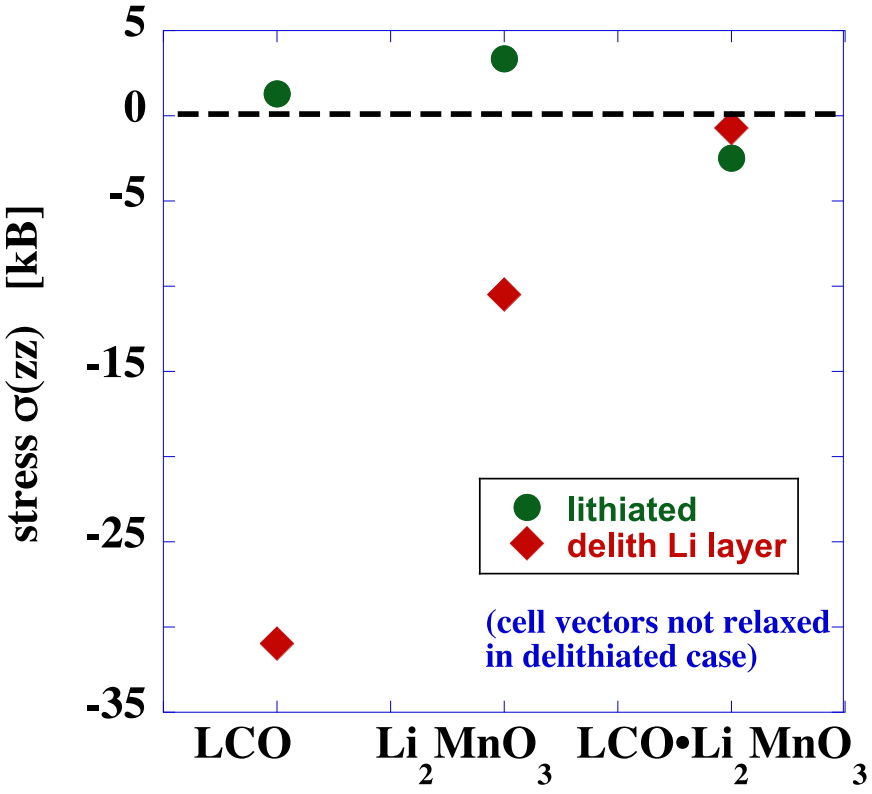

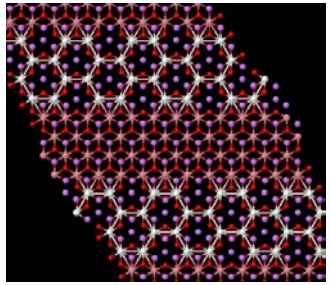

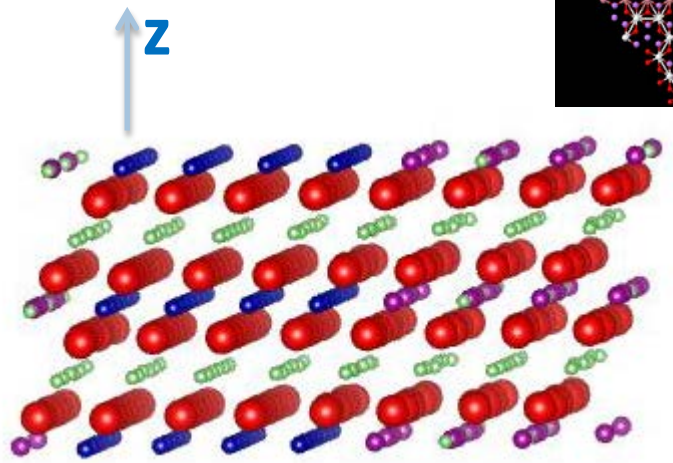

LCO Li_2MnO_3

Simplest model of composite: striped domains mimic some TEM observations

- c-axis stress induced by delithiation of composite lower than of separate phases
- composite prevents collapse of c-axis of LCO, which promotes extraction/insertion

Simulation of charge/discharge

- Charge: remove groups of Li at “random” sites (first in LCO, and then in Li_2MnO_3)
- Relax structure with (a) steepest descents [athermal], and/or (b) run AIMD at 1000K [simulate activated rearrangement]
- Discharge: relithiate interstices (“best-bonded sites”)
- Oxygen loss: fully oxygenated, or with V_O

First charge: fully oxygenated

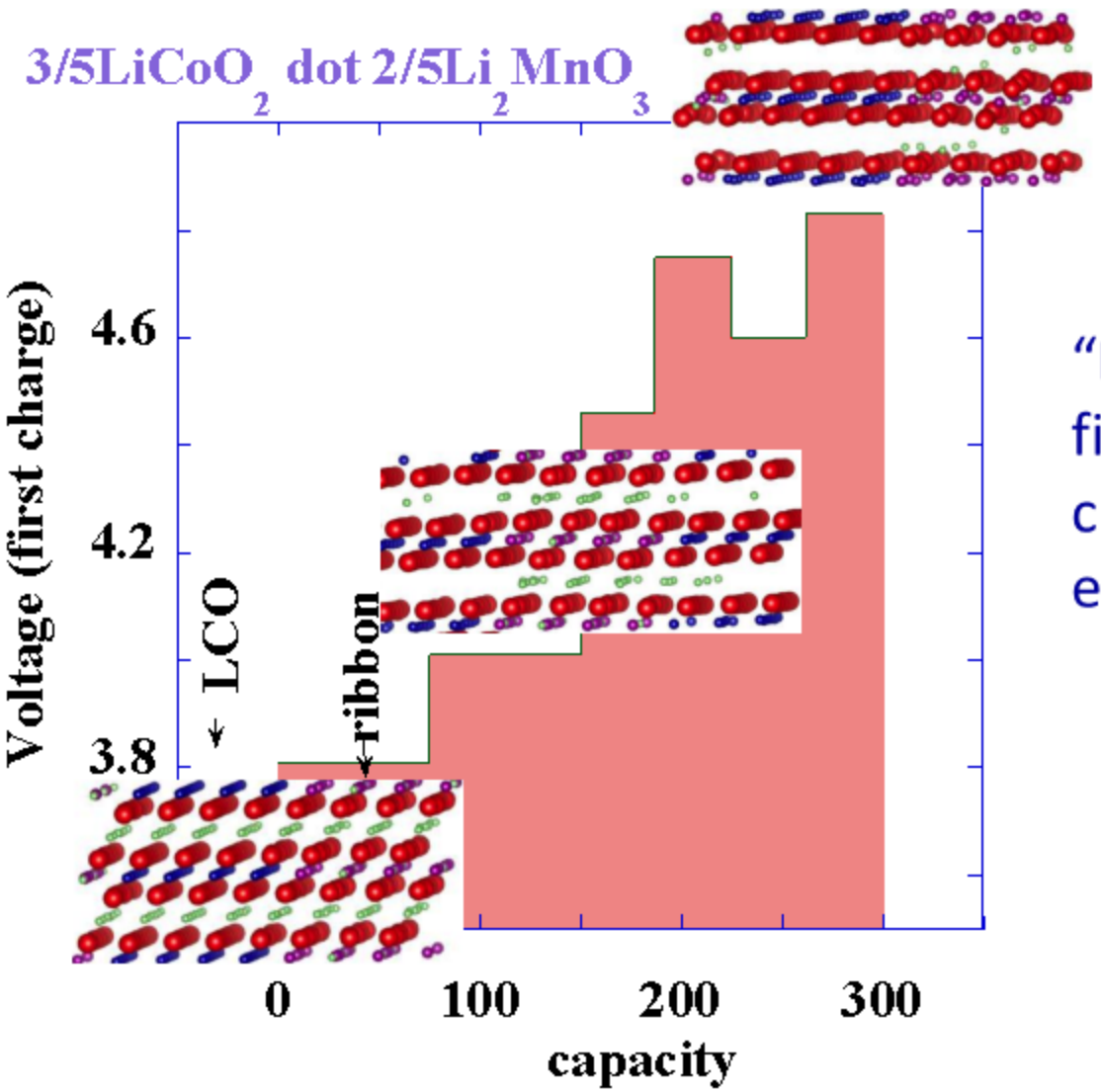

"Ribbon" structure gives first charge voltage curve consistent with experiment

First Charge + (part of) Discharge (O loss and thermal activation not included)

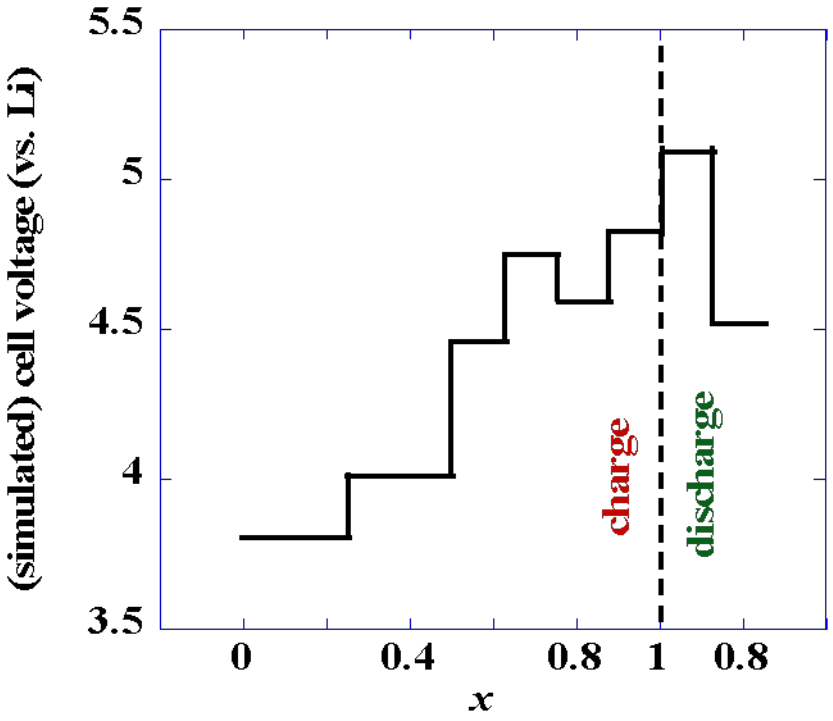

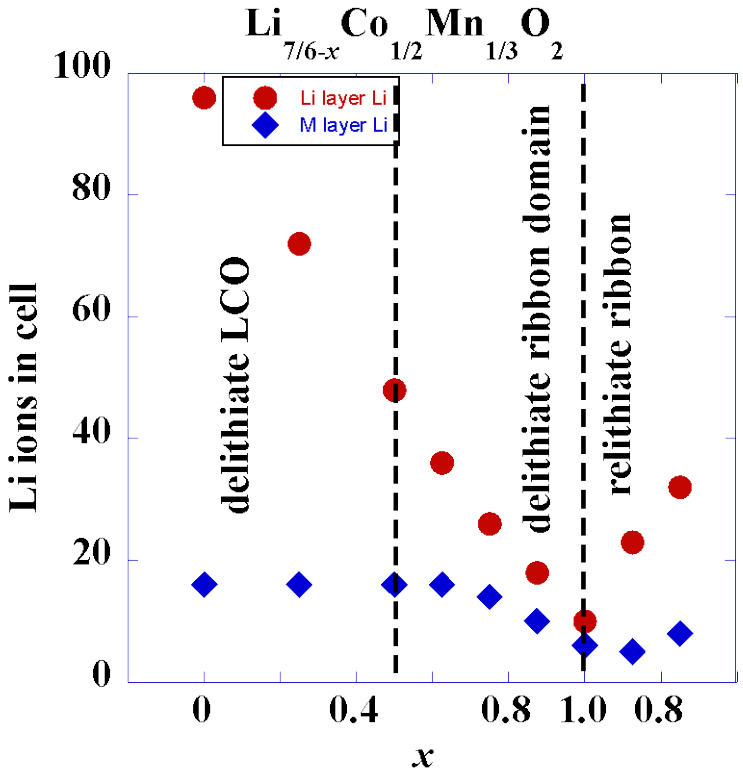

- Interlayer Li migration partly spontaneous, partly thermally activated
- With thermal activation included, M layer Li =0, at x=1
- AIMD helps achieve equilibration

Oxygen loss, tetrahedral Mn

Constraints: $\Delta CN(Mn) = -2n(V_O) - 2n(Mn_T)$

$n(V_O) \leq \frac{1}{2}\, n(V_{Li})$ [in domain]

Experiment:

CN(Mn) ≈ 5.4 at end of first charge (for NM comp)

[EXAFS (Croy et al., ES: 194)]

- (likely) implication: $n(V_O) \geq 0$; $n(Mn_T) \geq 0$
- More info required to determine $n(V_O)$, $n(Mn_T)$ individually

(approximate) constraint on $n(Mn_T)$: XANES Mn-K pre-edge $\mu_{K,pre}(Mn)$

- $\gamma = \mu_{K,pre}(Mn_T)/\mu_{K,pre}(Mn_O) \approx 5$ (from standards)
- $\mu_{K,pre}(SOC=x)/\mu_{K,pre}(pristine)$

  $\approx [\gamma\, n(Mn_T) + n(Mn_O)]/\,[n(Mn_T) + n(Mn_O)]$

Approximate soln. for NM [top of first charge]

(EXAFS, XANES from Croy et al. ES: 194):

$n(Mn_T) \approx 0.1$, $n(V_O) \approx 0.2$ (from eq. previous slide)

Simulations (next slide) suggest that for octahedral Mn ions with CN=4, $Mn_O \rightarrow Mn_T$

Influence of (0,1,2) oxygen vacancies on Mn octa-tetra migration

Mn location	O Vacancies in Mn coordination shell	$E(Mn_T)-E(Mn_O)$	E_{mig}
Li_2MnO_3 domain	0	+0.85	+
	1	+0.14	+0.98
	2	-0.09	+
Domain interface	0	+1.75	+
	1	+0.3	+0.95
	2	<0.0	0 (no activation required)

- With 2 oxygen vacancies [i.e., $CN(Mn_{oct})=6-2=4$], migration energetically favorable
- If $n(V_O) \geq \approx 0.1$, concentration of Mn with $CN(Mn_{oct}) = 4$ is appreciable, and nonzero $n(Mn_T)$ is expected (see also ORNL presentation on Mn_T)

Charge Compensation during first charge (schematic): $Li_{7/6-x}Co_{1/2}Mn_{1/3}O_{2(1-y)}$

$$x = 1/2\ n(Co^{4+}) + 1/3\ n(Mn^{5+}) + 2\ n(O^{-}) + 4y$$

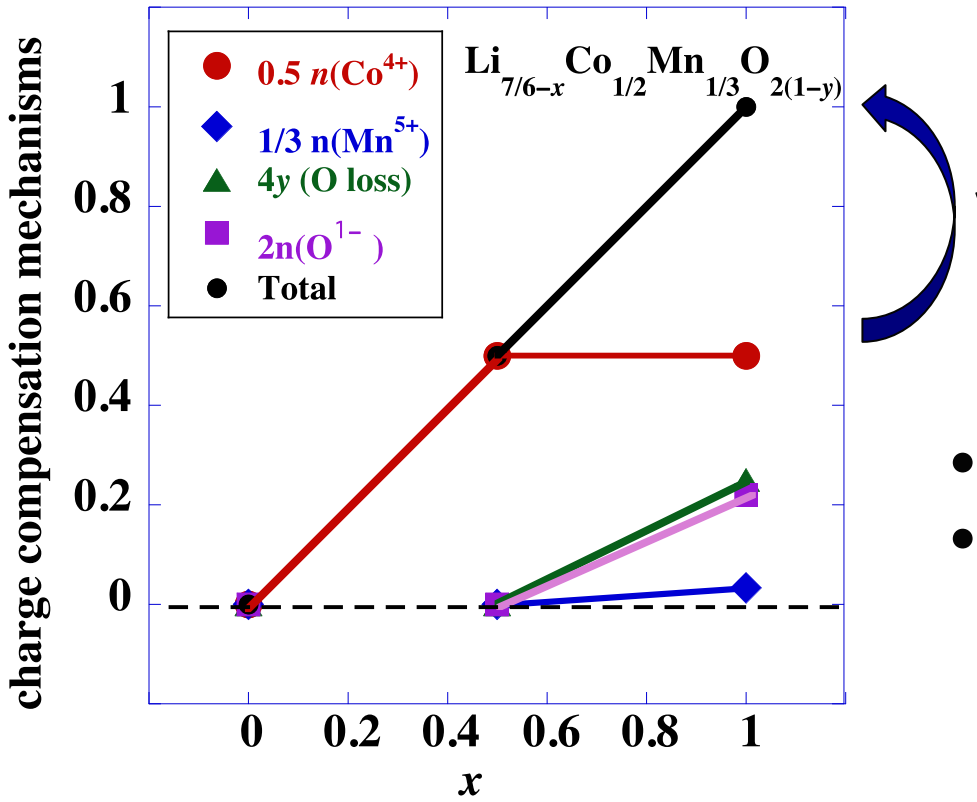

Vo,O^{-} & Mn^{5+}

- Co oxidized first (x<0.5)
- Mn oxidation, O-loss and O Oxidation may occur during activation (x>0.5)

signatures of local atomic arrangements in NMR spectra

Pristine material

- NMC ordering (see supplementary slides and Key et al. ES:187)
- Domain interface

Cycled material

- Tetrahedral Mn
- Low-coordination Li
- Domain interface

Predicting NMR shifts for different stable structures, using heuristic rules as derived by C. P. Grey and N. Dupré in: Chem. Rev. 2004, 104, 4493-4512

$LiCoO_2/Li_2MnO_3$ Ribbon (pristine)

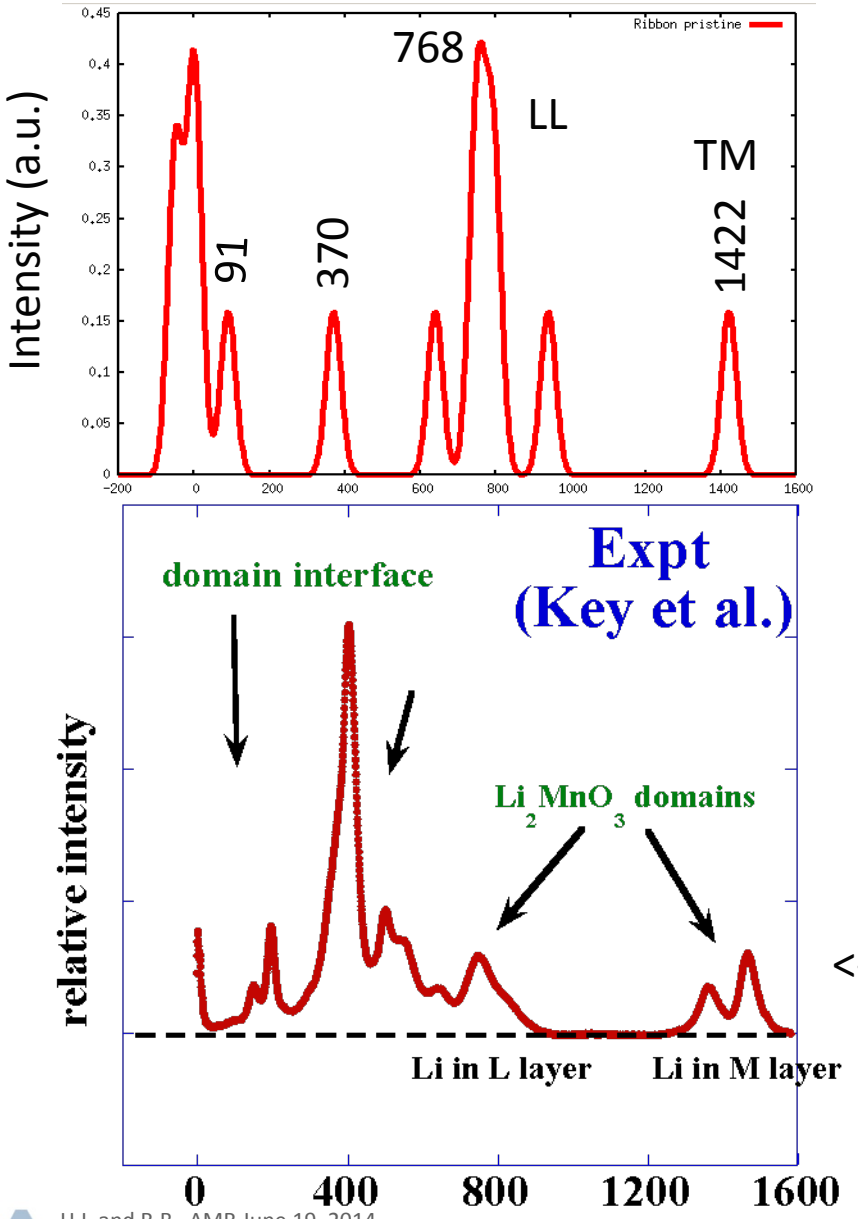

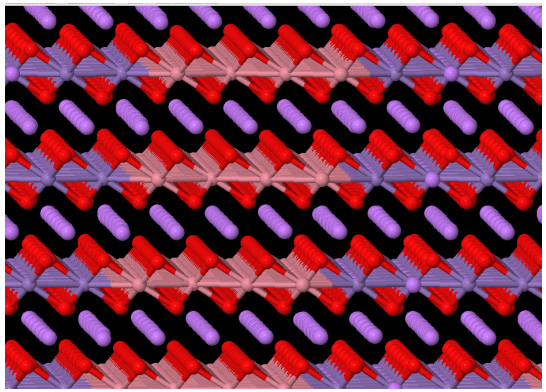

configurations contributing to NMR:
small shifts indicate few Li-O-Mn pathways
→ (domain boundaries)
Larger shifts (~750, 1450) are from domain interior

<-- 0.5-$LiCoO_2$:0.5- Li_2MnO_3

NMR modeling in collaboration with Russell J.T. (ANL)

$LiCoO_2/Li_2MnO_3$ Ribbon (delithiated and 12.5% O vac.)

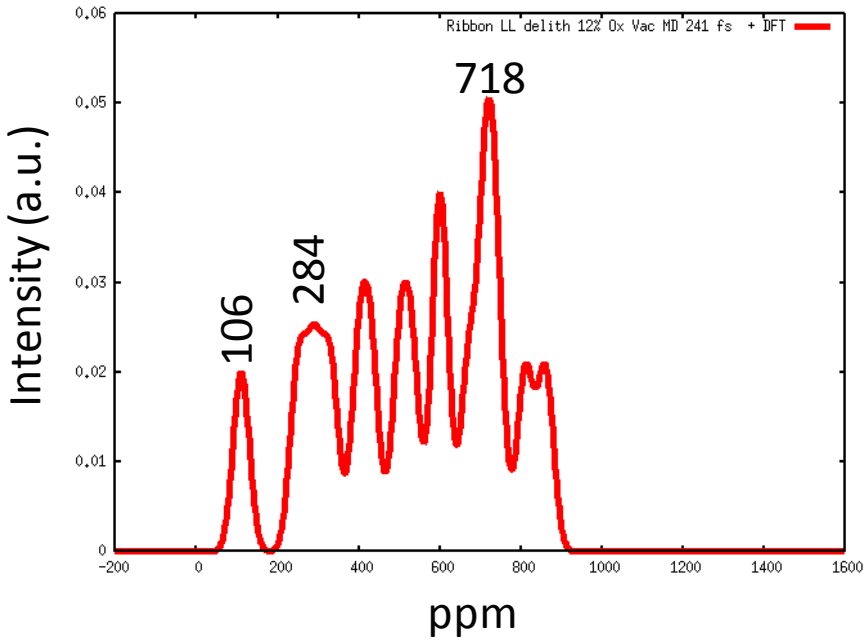

Mn in TT site

Co in TT site

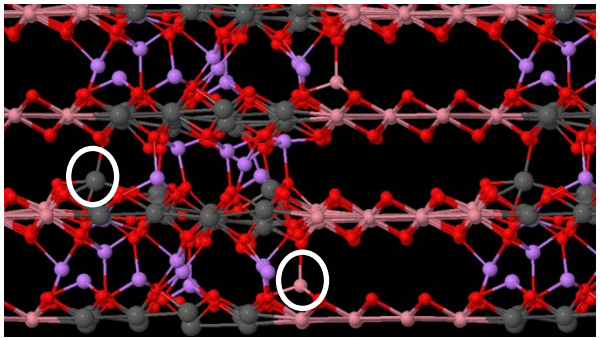

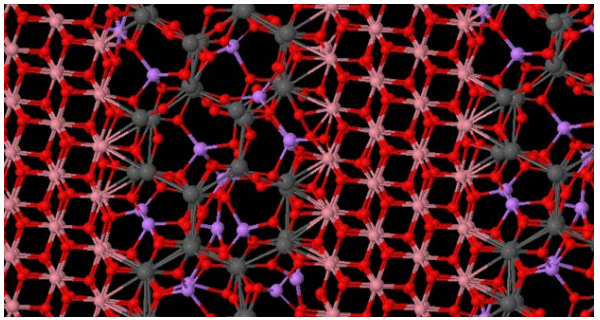

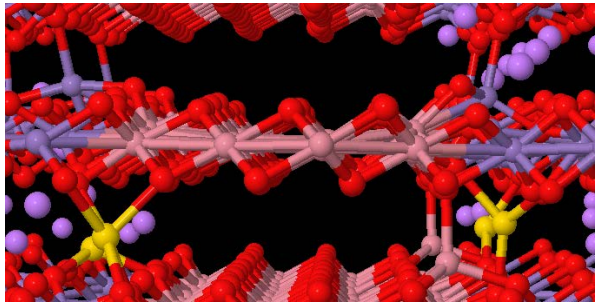

Atoms shown in gold are Li atoms with low NMR shifts: 106 and 284 ppm bands. Under-coordinated Li at the domain boundaries. consistent with experimental observations (see Key et al. ES 187)

Tetrahedral Li in Li_2MnO_3 domain contribution to NMR signal (broadening to low ppm). Also consistent with ORNL neutron diffraction experiments, that show TT Li.

XANES spectra for tetrahedral Mn

Is tetrahedral Mn 5^+?

- Simulated tetrahedral Mn in $Li_{2(1-f)}MnO_3$:
  5^+ for U_{eff} = 4 eV
  4^+ for U_{eff} = 5 eV
  (U_{eff} is Hubbard parameter)

- Enhanced pre-edge simulated in either case

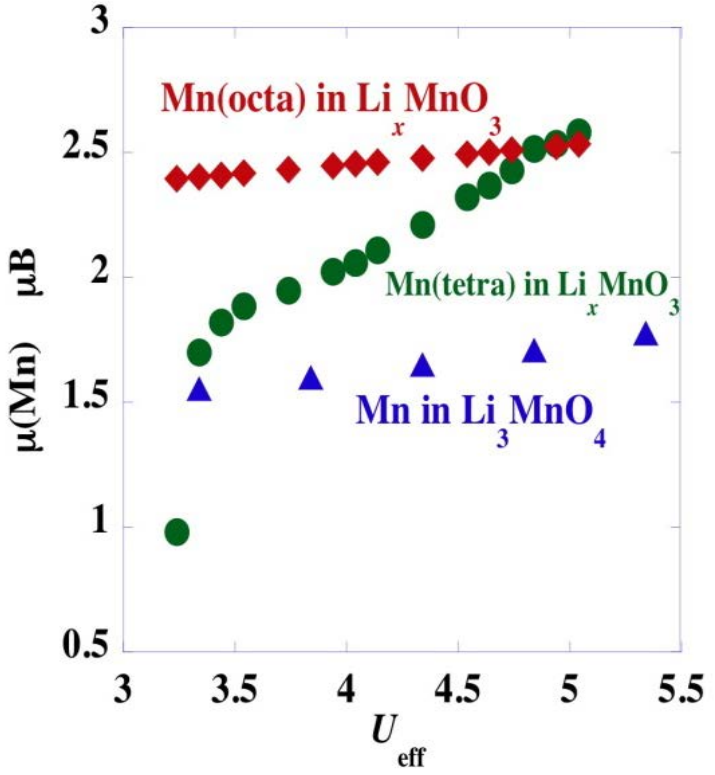

Li_2MnO_3 Bulk (3-Li & 1-O vac. Mn in tet. site) Mn-K edge

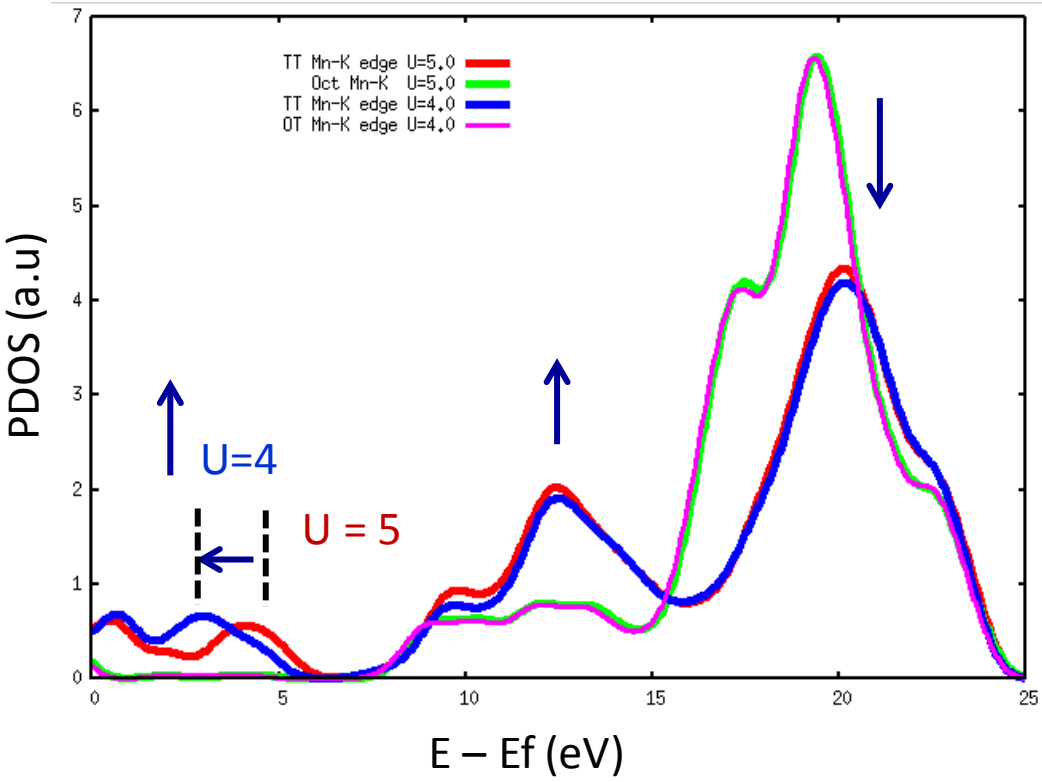

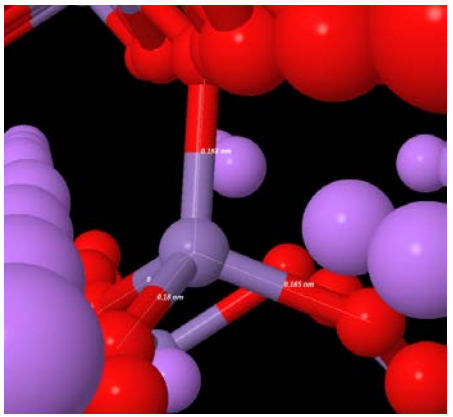

TT Mn (3 Li and 1 O vac. 688 cell)

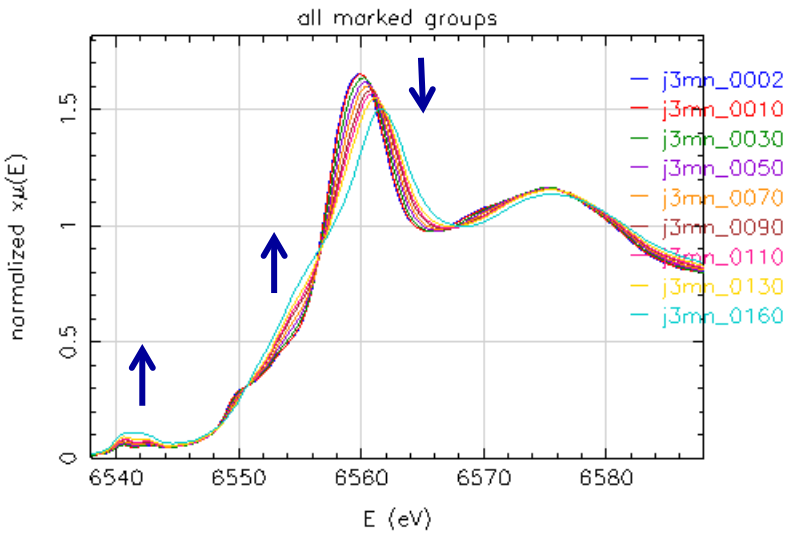

The intensity of Mn-K pre-edge is increased w.r.t octahedral Mn^{4+} in Li_2MnO_3: consistent with Li_3MnO_4 standard, XANES (Croy et al ES 194). Shift of the Mn pre-edge with U=4? → Need more accurate method

Measured XANES (NiMn) (Croy et al. ES 194)

(proposed) event-chain leading to VF

1. Activation ➔ finite $n(V_O)$ (EXAFS)
2. Finite $n(V_O)$ ➔ $Mn_O(CN=4)$
3. $Mn_O(CN=4)$ ➔ $Mn_T(CN=4)$ [w or w/o thermal activation]
4. $Mn_T(CN=4)$ ➔ further transformations to structures that result in fade

Conclusions

- Oxygen vacancies, tetrahedral Mn appear likely
- Mutual stabilization effect of Li_2MnO_3 and $LiCoO_2$ in the composite
- Athermal (as well as activated) tetrahedral Li formation in the LL with cycling
- EXAFS and NMR provide constraints to guide simulations of charge and discharge

Acknowledgements

Burrell, Anthony K.; Abouimrane, Ali; Abraham, Daniel; Amine, Khalil; Balasubramanian, Mahalingam; Bareno Garcia-Ontiveros, Javier; Belharouak, Ilias; Benedek, Roy; Bettge, Martin; Bloom, Ira D.; Long, Brandon R.; Chen, Zonghai; Croy, Jason R.; Dees, Dennis W.; Dogan, Fulya; Gallagher, Kevin G.; Henriksen, Gary L.; Iddir, Hakim; Ingram, Brian J.; Johnson, Christopher; Key, Baris; Li, Yan; Lu, Wenquan; Miller, Dean J.; Ren, Yang; Slater, Michael D.; Thackeray, Michael M.; Vaughey, John T.; Wu, Huiming; Wu, Qingliu; Zhu, Ye; Yang, Zhenzhen; Lee, Eungje; Aoun, Bachir; Vu, Anh D.; Lin, Chi-Kai; Rinaldo, Steven G.

- Support for this work from DOE-EERE, Office of Vehicle Technologies is gratefully acknowledged
  - David Howell, Peter Faguy & Tien Duong

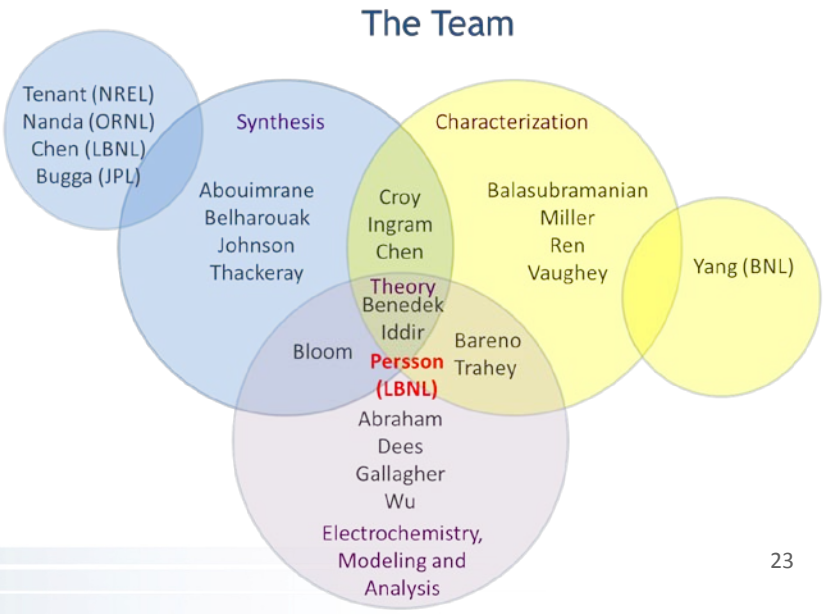

Future Work - Rest of FY 2014

- Continue simulation of discharge (ribbon model, and Li_2MnO_3)
- Complete migration studies, tetrahedral Mn, and disseminate results in publications (in preparation with Croy J. et al.)
- Complete simulation of ribbon model, and disseminate results in publications

Technical Back-Up Slides

Li_2MnO_3 Bulk (3-Li & 1-O vac. Far from tet. Mn site): Mn-K edge

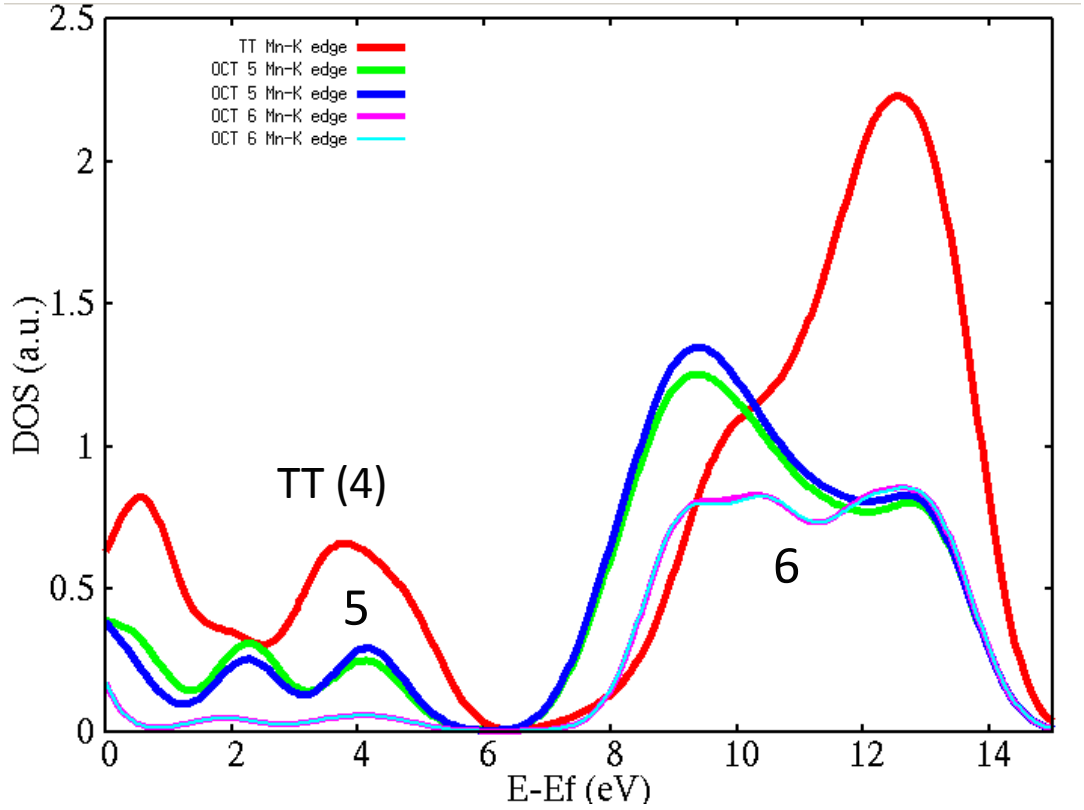

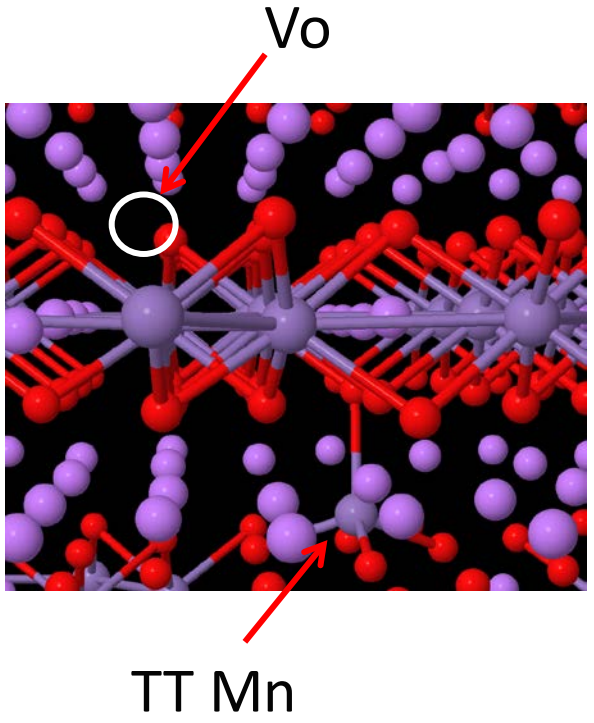

- Increase intensity of the Mn-K pre-peak for lowe Mn-O coordination
- Mn-K pre-peak shape: symmetry dependent

$LiCoO_2$: Co vacancy migration (M → M)

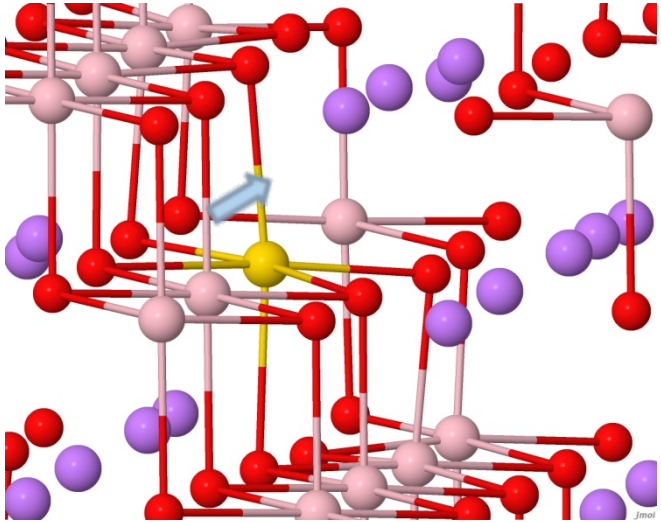

Initial position: Migrating Co is shown in yellow, and the migration path in blue

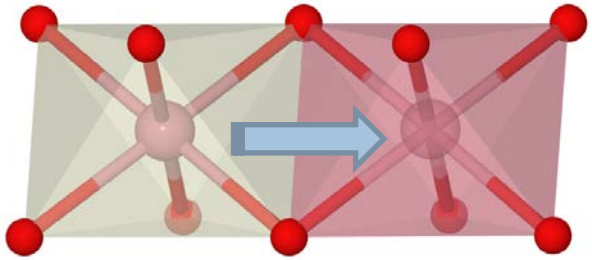

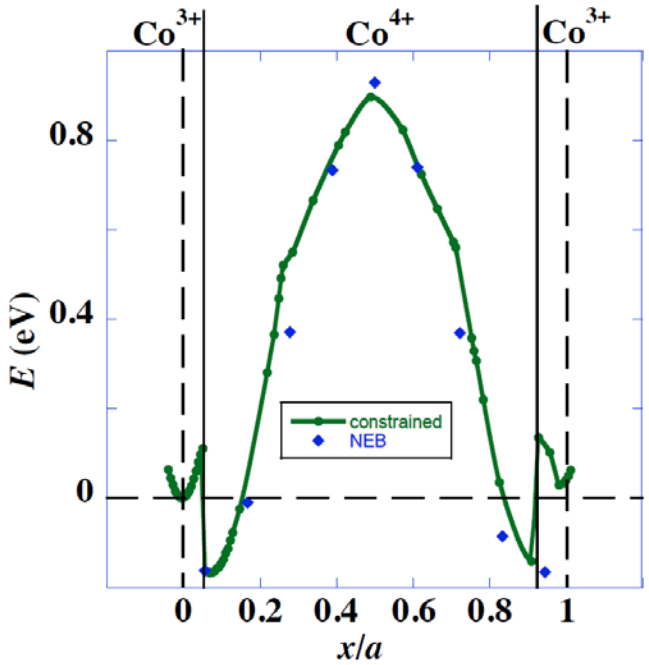

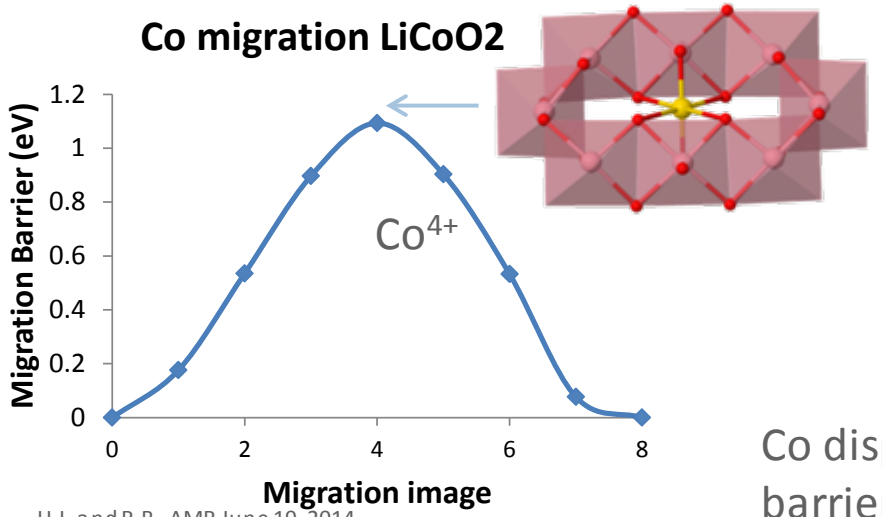

Co disproportionation, lower the migration barrier.

$Li_{12}Ni_4Mn_4Co_4O_{24}$
Exploring lowest energy configurations for cluster expansion calculations

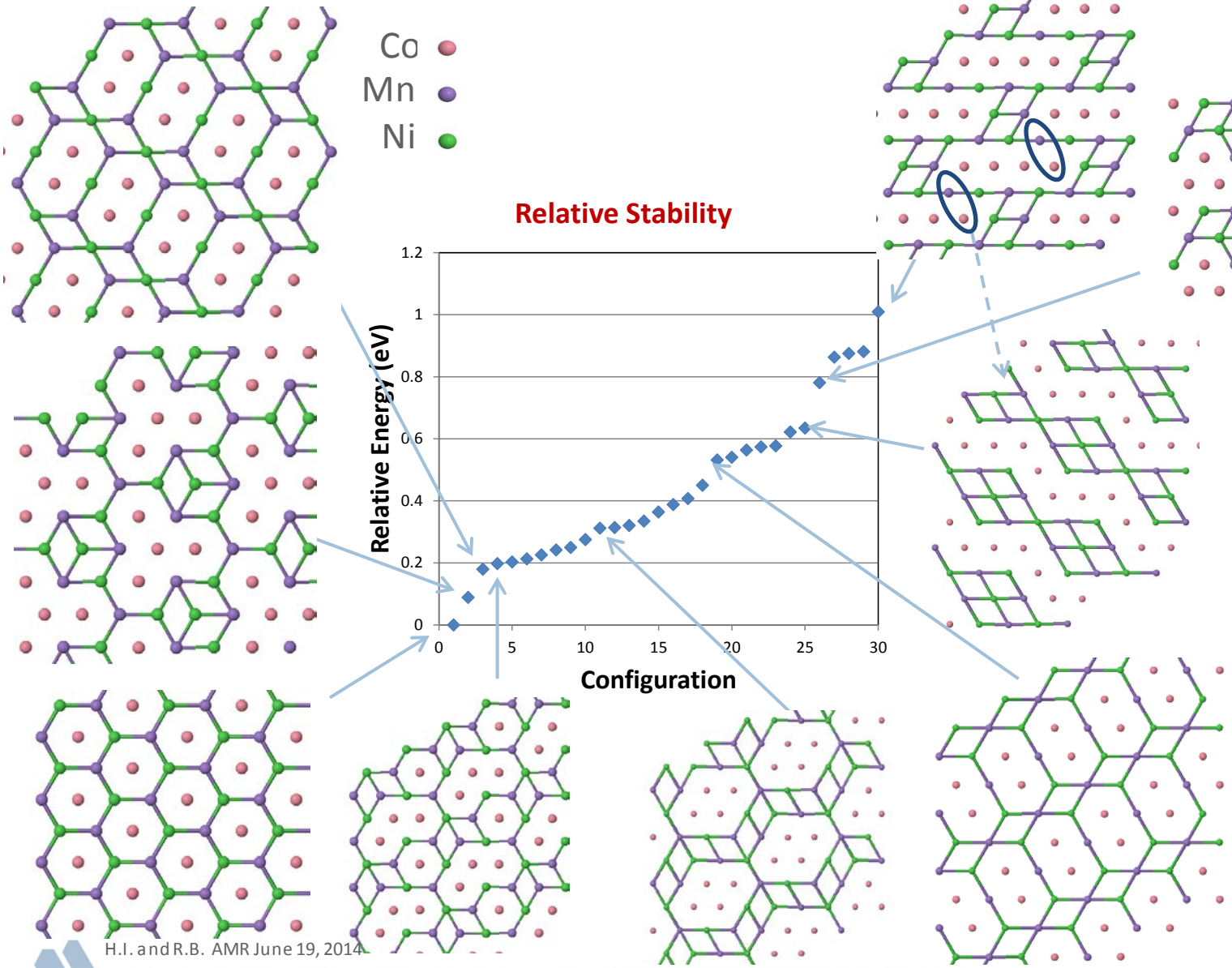

DFT order	Name	Relative E (eV)
1	con0-741	0.000
2	con0-29	0.089
3	con0-740	0.179
4	con0-739	0.198
5	con0-727	0.204
6	con0-736	0.213
7	con0-742	0.227
8	con0-405	0.242
9	con0-396	0.251
10	con0-369	0.275
11	con0-724	0.312
12	con0-737	0.314
13	con0-735	0.323
14	con0-733	0.334
15	con0-732	0.364
16	con0-341	0.388
17	con0-655	0.409
18	con0-416	0.475
19	con0-794	0.533
20	con0-344	0.540
21	con0-710	0.565
22	con0-721	0.574
23	con0-659	0.578
24	con0-718	0.622
25	con0-609	0.635
26	con0-756	0.780
27	con0-766	0.863
28	con0-768	0.881
29	con0-789	0.885
30	con0-769	1.009

Contribution to total NMR spectra from 22 configurations of NMC333

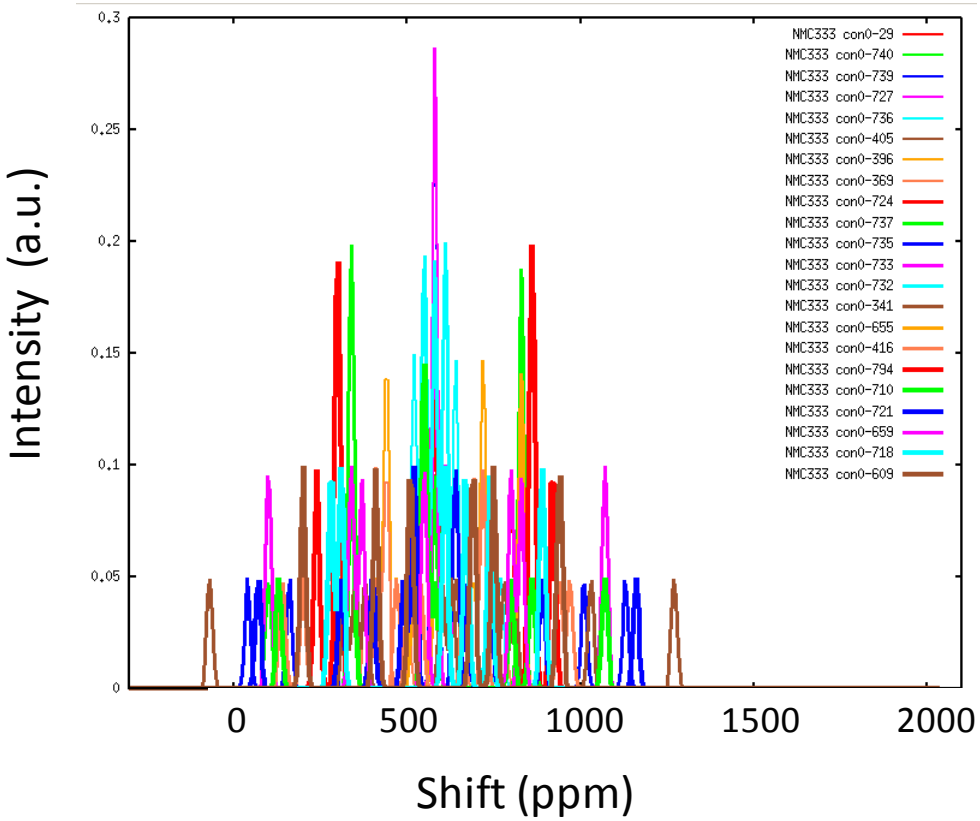

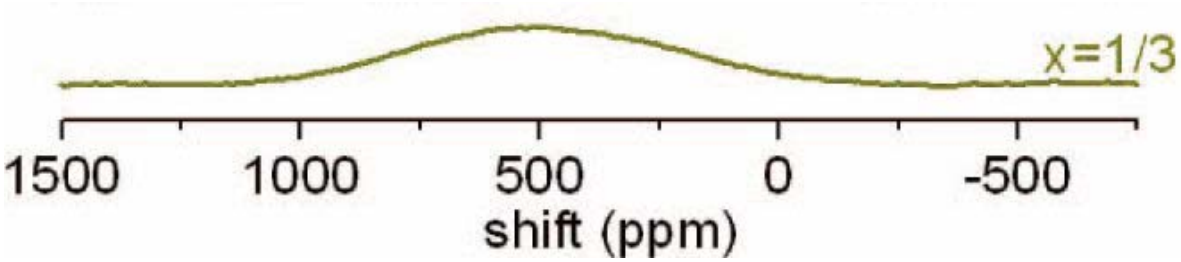

Exp. NMR from D. Zeng et al., Chem Mat., 2007

Predicted NMR shifts from $LiMn_2$ domains

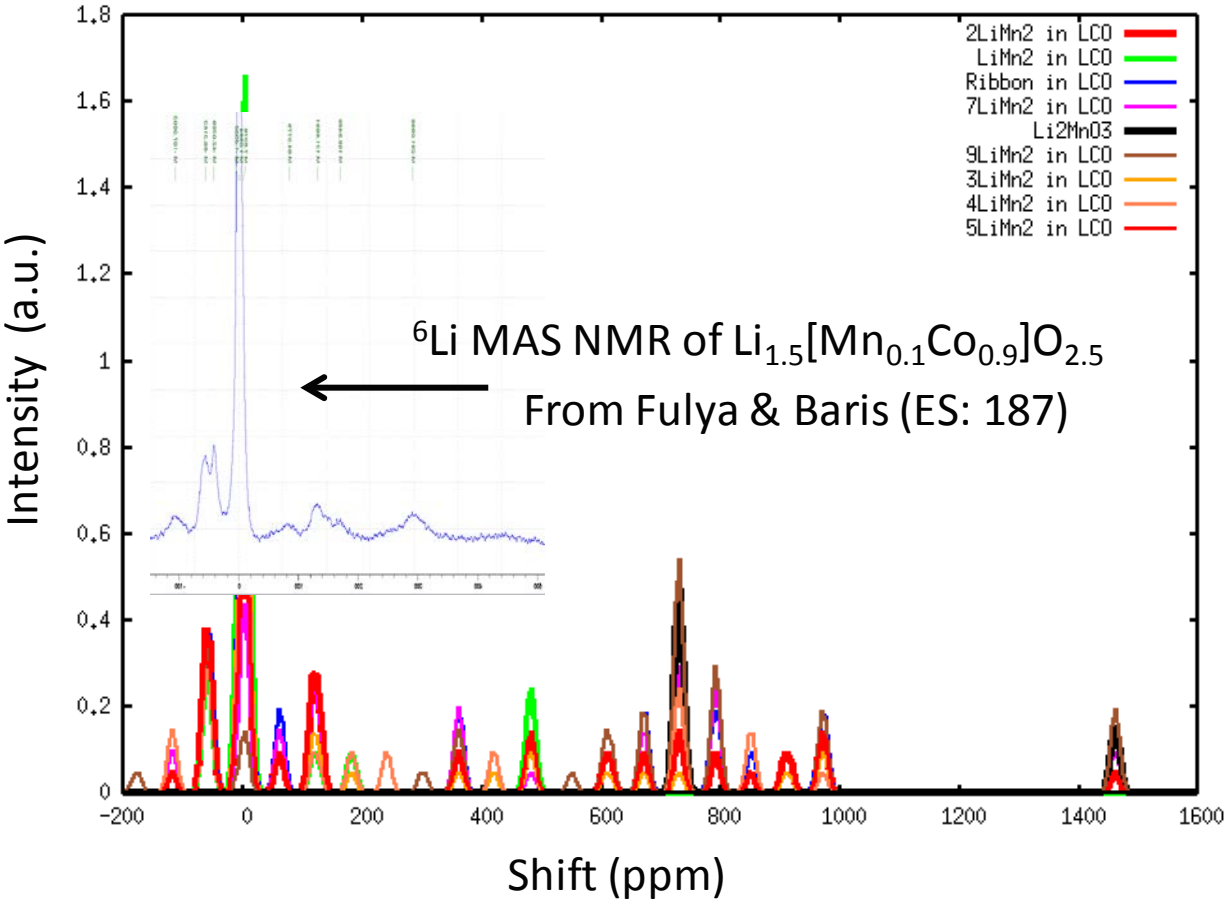

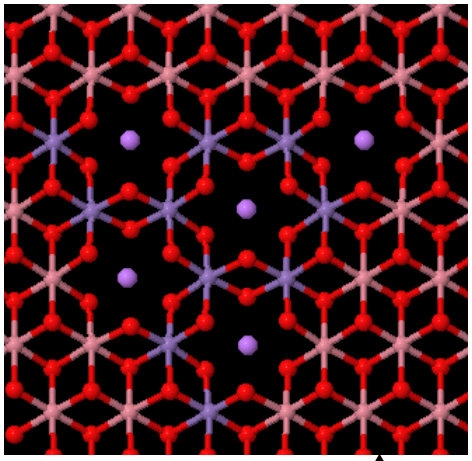

5 $LiMn_2$ units

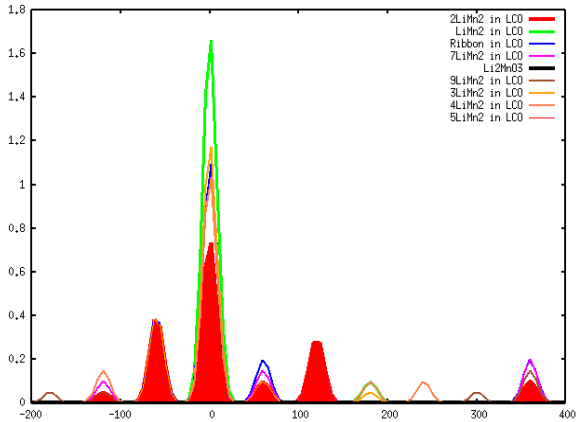

Identification of possible configurations contributing to NMR shifts for small $LiMn_2$ domains, such as in $Li_{1.5}[Mn_{0.1}Co_{0.9}]O_{2.5}$

Filled area (red) NMR contribution from a cluster of 5 LiMn2 units